Digital Twin-based Framework for Heat Stress Calculation

Iván Cárdenas-León[1], Rodrigoandrés Morales-Ortega [1], Mila Koeva[1], Funda Atún[1], Karin Pfeffer[1]

[1]Faculty of Geo-Information Science and Earth Observation (ITC), University of Twente, Enschede, NL
- (i.l.cardenasleon, l.r.moralesortega, m.v.koeva, f.atun, k.pfeffer)@utwente.nl

Keywords: Physiological Equivalent Temperature, Urban Heat Islands, Heat Stress, Digital Twins

Abstract

According to the KNMI Klimaatsignaal’21, the average surface temperature in The Netherlands has increased by 2.3°C between 1901 and 2020. Moreover, The Netherlands is also experiencing more frequent and intense heatwaves. Urban development significantly impacts the environmental conditions of a city, influencing thermal comfort and human well-being. To deal with these problems, municipalities across the country have been tasked to find ways to measure, understand, and find solutions to the increasing temperatures, specifically in urban areas. Because of this, several contrasting urban heat maps have been produced using different metrics and methods by different agencies. Koopman et al. presented a methodology for a standardized urban heat map at a 1-m spatial resolution to unify the stress tests by selecting the Physical Equivalent Temperature (PET) as a metric for heat stress. The PET is a key indicator in bio-meteorology, quantifying the combined effects of various environmental factors on human thermal perception. Despite its utility, widespread adoption of PET-based assessments by municipalities remains limited. To address this gap, this paper presents the development of a Digital Twin framework using PET analysis, enabling a collaborative, nondestructive, and cost-effective assessment of urban interventions’ impact on thermal conditions. Leveraging geoprocessing workflows and geospatial data, our framework allows for real-time PET calculations and scenario testing, facilitating informed decision-making by urban planners. The framework was tested and applied for Enschede, Netherlands, demonstrating its efficacy in visualizing current conditions, projecting future scenarios, and evaluating intervention strategies. Feedback from urban planners highlighted the tool’s usability and potential for enhancing community engagement in urban planning processes.

1. Introduction

Urban development modifies the environmental characteristics of radiation, temperature, humidity, and aerodynamics of a city (McGregor et al., 1998). Rapid urbanization, climate change, and a growing awareness of the impact of environmental conditions on human well-being (Tong et al., 2021; Flynn et al., 2005) have influenced the need to accurately assess thermal comfort, gaining significant prominence in current years (Das and Subudhi, 2022; Zou and Zhang, 2021).

A human body feels comfortable when it can quickly gain thermal balance with the surrounding environment (Das and Subudhi, 2022). As this balance is also dependent on individual conditions such as metabolic rate, transpiration, activity level, clothing, gender, and age (Höppe, 1993), different agencies and researchers have produced various contrasting urban heat island mapping methods with different metrics, such as the number of warm nights (Jain, 2023), Land surface temperature (Zhao et al., 2024; Kasniza Jumari et al., 2023), and Surface Urban Heat Island Intensity (Xi et al., 2024; Pauly et al., 2024; Di Bernardino et al., 2023). Additionally, (Sidiqui et al., 2022) analyzes risk mapping and vulnerability assessment using GIS geospatial data, considering the population of Greater Geelong, Australia.

Valmassoi and Keller (2021) use different approaches to visualize the Urban Heat Island (UHI) effect by selecting a rural reference location and the follow-up comparison with the urban area. (1) Single Point Baseline: Utilizes a single rural location as the reference point for temperature comparison; (2) Area Averaged Baseline: Averages temperatures over a specified rural area to establish the baseline;(3) Nearest Neighbor-Based Baseline: Employs the closest rural temperature data point to each urban grid point for comparison. After comparing the results, it was identified that while all methods are reasonable approximations of the UHI, they are also prone to biases and under/overestimating the phenomena.

Likewise, cities across the Netherlands have studied heat stress using several methods that differ from place to place. For instance, in Utrecht, Brandsma and Wolters (2012) measured the nighttime UHI intensity at street level using sensors installed on bicycles and studying the Sky-view Factor and cloud coverage effects. In The Hague, Koopmans et al. (2018) studied the number of tropical nights in different climate scenarios. In Rotterdam, Klok et al. (2012) used the Land surface temperature to indicate surface heat island, comparing data from 1984 to 2007. Therefore, due to different variables, sources, and methods, comparing results from different approaches has become increasingly complex, creating the need for a unified, standardized solution.

To unify the stress tests, Koopmans et al. (2020) presented a methodology for urban heat stress at 1-m spatial resolution in the Netherlands. Their research proposes using the Physiological Equivalent Temperature (PET) as a standardized indicator. PET is a key indicator in bio-meteorology that quantifies the combined effects of air temperature, humidity, wind speed, and solar radiation on human perception of thermal conditions (*ibid*). The PET indicator is the outdoor air temperature equivalent of an indoor setting on a person with 80W of metabolism, light activity, and wearing a suit (clothing factor of 0.9) (Höppe, 1999). According to this indicator, several grades of stress are present, as shown in Table 1.

Some researchers have already included PET as an indicator for comfort in academic studies (Çağlak, 2024; Zhang et al., 2022; Feng et al., 2024). And, despite the understanding and standardization in the Netherlands that this indicator has brought to urban planners, it is still not widely adopted by municipalities and other sub-national governments which struggle to find ways to integrate standard methods with their workflow (Koopmans et al., 2020).

https://doi.org/10.5194/isprs-annals-X-4-2024-67-2024

PET	Thermal Sensitivity	Grade of Physiological Stress
<4 °C	Very cold	Extreme cold stress
4 - 8°C	Cold	Strong cold stress
8 - 13 °C	Cool	Moderate cold stress
13 - 18 °C	Slightly cool	Slight cold stress
18 - 23 °C	Comfortable	No thermal stress
23 - 29 °C	Slightly warm	Slight heat stress
29 - 35 °C	Warm	Moderate heat stress
35 - 41 °C	Hot	Strong heat stress
41 - 47 °C	Very hot	Extreme heat stress
>47°C	Scorching	Most Extreme heat stress

Table 1. PET, Thermal Sensitivity and Grades of Physiological Stress. Adapted from (Matzarakis and Mayer, 1996)

In recent years, research in participatory tools has shown their importance in enhancing and facilitating citizen participation in action planning (Flacke et al., 2022) and stakeholder engagement in collaborative spatial planning processes (Aguilar, 2022). Therefore, following this line of thinking, a Digital Twin as a participatory tool is presented in this research. It aims to facilitate understanding, interaction, and collaboration processes between stakeholders, allowing them to easily propose and share ideas in real-time with others in person or online.

According to the Digital Twin Geohub (2022), a digital twin (DT) is a dynamic digital representation of a physical object or system. It integrates data from various sources, including sensors and analytics, to mirror the real-world state of the object or environment. This allows for real-time monitoring, simulation, and decision-making. Initially used in manufacturing, DT has expanded into geospatial domains, representing not just the geometry but also the behavior and evolution of living environments. It's a tool encompassing technologies like GIS, IoT, AI, and VR to create a comprehensive and interactive model of physical reality. An Urban DT is a replica of the physical elements of a city that can be used to co-create and test different scenarios on city-specific parameters (Ruohomaki et al., 2018). It is not an exact copy, as it also serves as a container for models, data, and simulations (Dembski et al., 2019). DTs can potentially address the complex challenges of cities while involving citizens within the planning process (Dembski et al., 2019).

This paper presents a Digital Twin-based framework that uses the PET indicator as a base. The framework allows urban planners and governmental organizations to interact in a collaborative, nondestructive, and inexpensive digital georeferenced environment to identify the effects of the changes on the location, size, and quantity of green (grass, natural surfaces, and trees), blue (water courses or ponds), and gray infrastructures (buildings). The DT allows the generation of a map in near-real time with the changes and suggestions done by urban planners in a GIS environment. This research aims to answer the following questions: *How do small local interventions affect PET values?* and *How can different interventions on urban landscape be tested ex-ante?*

2. Materials and Methods

The study area of this research corresponds to the city of Enschede in the Netherlands. Enschede is one of the biggest cities in the Netherlands, with a population of around 160.000 inhabitants (CBS, 2024). The city possesses a compact central business district (CBD) and transitions to a more open peri-urban residential area. The inner urban area includes parks and water bodies for recreation. An industrial port and university campus are on the city's western side.

The design of the DT started with a direct collaboration with the Enschede Municipality. Members of staff and daily decision-makers indicated the need to easily identify empty locations with high heat stress that require interventions. To achieve this, as a component of the DT, the building footprints openly available from the so-called Basic Address Registration (BAG) data have been used (Dataset: Basisregistratie Adressen en Gebouwen , BAG). 2D footprints, instead of the 3D LOD2 objects, were used to allow easy editing and reduce processing times. In addition, the LiDAR scanning from the city was downloaded from the national open-source platform "Current elevation file in the Netherlands" (Dataset: Actueel Hoogtebestand Nederland 4 , AHN). The LiDAR scanning data was used for the Digital Terrain Model (DTM) and Digital Surface Model (DSM) generation to determine the buildings, tree heights, and tree crown configuration. Moreover, the Normalized difference vegetation index (NDVI) average month values from the hottest month recorded in 2018-2019 were obtained from Sentinel-2 Satellite Imagery (Copernicus Sentinel Data, 2023) via Google Earth Engine(Gorelick et al., 2017). The water bodies were supplied by the Enschede municipality Geoinformation department and were complemented with polygons obtained from OpenStreetMaps (OpenStreetMap contributors, 2023); this complement was selected as a way to ensure reproducibility in other contexts with less data availability. These elements allowed the whole city to be reconstructed in a digital environment in 2D and 3D. The summary of input data is presented in Table 2.

The PET DT was designed to include the spatial dataset input in a 2D visualization for easy operation. There, it is possible to have tools that allow for adding geographical features, such as buildings, green areas, water bodies, and the inclusion of trees, to observe the consequences of adding or removing new features/elements such as water bodies, buildings or green infrastructure on the PET values. The modifications are recorded in a cloud spatial database and displayed in real-time in the 2D and 3D visualizations. The calculation of the PET value follows the standardized method on a 1-m spatial resolution for the Netherlands developed by Koopmans et al. (2020), which was developed on measures and calculations on the city of Wageningen as shown in Equation 1. The calculation result can then be downloaded in a Raster file where pixel values indicate the expected PET at each location. The overall process can be seen in Figure 1.

$$\begin{aligned} PET_{sun} = & -13.26 + 1.25T_a + 0.011Q_s - 3.37\ln(u_{1.2}) \\ & +0.078T_w + 0.0055Q_s\ln(u_{1.2}) + 5.56sin(\varphi) \\ & -0.0103Q_s\ln(u_{1.2})sin(\varphi) + 0.0546B_b + 1.94S_{vf} \end{aligned} \quad (1)$$

where
T_a = air temperature ($°C$) at 2m
Q_s = solar irradiation (W/m^2)
$u_{1.2}$ = wind speed at 1.2m height (m/s)
T_w = wet-bulb temperature
φ = solar elevation angle (degrees)
B_b = Bowen Ratio
S_{vf} = Sky-view factor

The calculation of the PET was integrated into a geoprocessing workflow developed to determine the PET value and be able to recalculate the value on changing meteorological, green, and blue

Geospatial Dataset	Specifications	Data Type	Date	Source
Building Footprint	Basic Registration Buildings	Vector Polygons	May, 2023	(Dataset: Basisregistratie Adressen en Gebouwen , BAG)
LiDAR Scanning	Aerial laser Scanning 10-14 points/m^2. Vertical accuracy 5cm	LAS	2022	(Dataset: Actueel Hoogtebestand Nederland 4 , AHN)
NDVI	Sentinel-2 average monthly pixel value. 10m spatial resolution	Raster Layer	July, 2019	(Copernicus Sentinel Data, 2023; Gorelick et al., 2017)
Trees	Public trees location	Vector Point	Jan, 2023	(Gemeente Enschede, 2023)
Water bodies	Canals, lakes, ponds	Vector Polygons	March, 2023	(Gemeente Enschede, 2023; OpenStreetMap contributors, 2023)
Meteorological Data	Hourly Temperature, humidity, wind speed and Solar radiation	Numerical	25th July, 2019	(KNMI, 2019)

Table 2. Datasets used

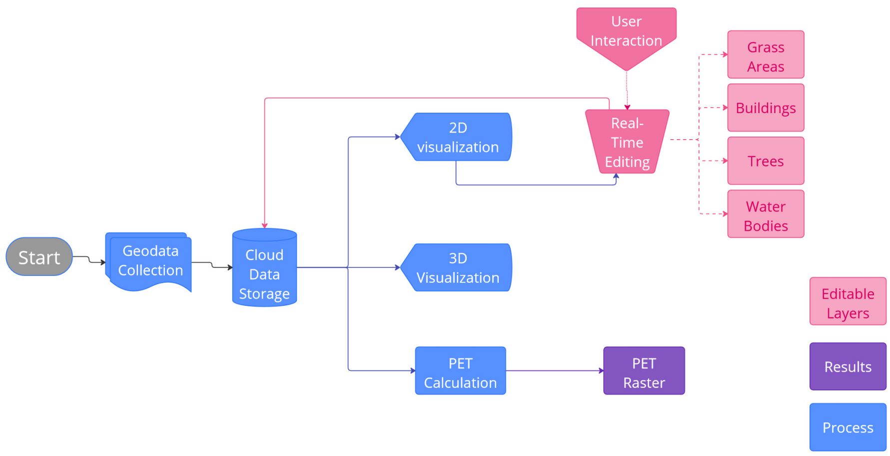

Figure 1. Digital Twin development overview process. Items in Magenta can be edited by user interaction

infrastructure or constructing a new building. Figure 2 summarizes the workflow, highlighting the elements of the environment that can be modified and the affected parameters when calculating the PET.

To explore different scenarios and allow stakeholders and citizens to propose local changes at the neighborhood level, an open-source Phyton code was developed to recalculate the solar angle and wet bulb temperature when specific meteorological conditions are set (See Solar angle code and Wet bulb code).

By default, the conditions from the 25th of July 2019 were used, as this day was the maximum temperature recorded in Twente Weather station (6.891°E 52.274°N, 34.80 m elevation) on the 2018 - 2023 period. The conditions on that day, at 14:00 h, were a temperature of 40.2°C, wind speed of 2m/s at a direction of 100°, Relative humidity of 47%, and Solar radiation of 259 J/cm^2. The wind simulation and the effects buildings and trees have on its flow were recalculated at 1.2m height using the WindNinja Tool (Forthofer et al., 2014) as the weather station measures at a 10m height in an open field.

For calculating the Sky View Factor (SVF), a measurement of the extent to which the sky can be seen without being obscured by nearby structures, trees, or other objects, an updatable DSM (Digital Surface Model) is required as it contains both the environment's natural and built/artificial features. A Raster Calculation was utilized to update the DSM, employing conditionals to incorporate the updates. This process allows user interaction with building configurations, enabling them to create and evaluate their environmental scenarios. New buildings can be drawn by hand, and a height can be specified, as this will affect the SVF. Due to building materials' high heat transfer capacity, the new building's Bowen Ratio is set to 3.

Due to the capacity of trees to provide shade, individuals experience a lower temperature, and trees act as natural wind barriers. It was important to test the effects of adding trees to unvegetated areas and help find the most efficient configuration. To do so, it became necessary to replicate the height, volume, and leaf crown structure of existent trees from the south and center of the city. Thus, to allow the experimental addition of *non-existent* trees on demand by the users, the tool enables users to choose between a 6m and a 24m height tree as a proof-of-concept and allows the users to load their tree layers to expand the usage of the tool depending on their specific needs and context.

A Python script was developed to load a polygon that represents a tree crown with its height values and use it to duplicate or*stamp* that tree polygon on each point of a point layer adjustable by the user (Figure 3). The trees are stored in an output polygon feature that is geo-referenced and ready to be rasterized and combined into the overall geoprocessing calculation.

Additionally, the inclusion of blue and green has the potential to reduce the heat transfer to the air. These elements were set to be drawn in a polygon with free-hand tools, and their Bowen ratio was set to 0.1 for water and 0.3 for green areas (grass). As with buildings, the resulting raster is combined with the original DSM using the raster calculator conditionals, where different pixel

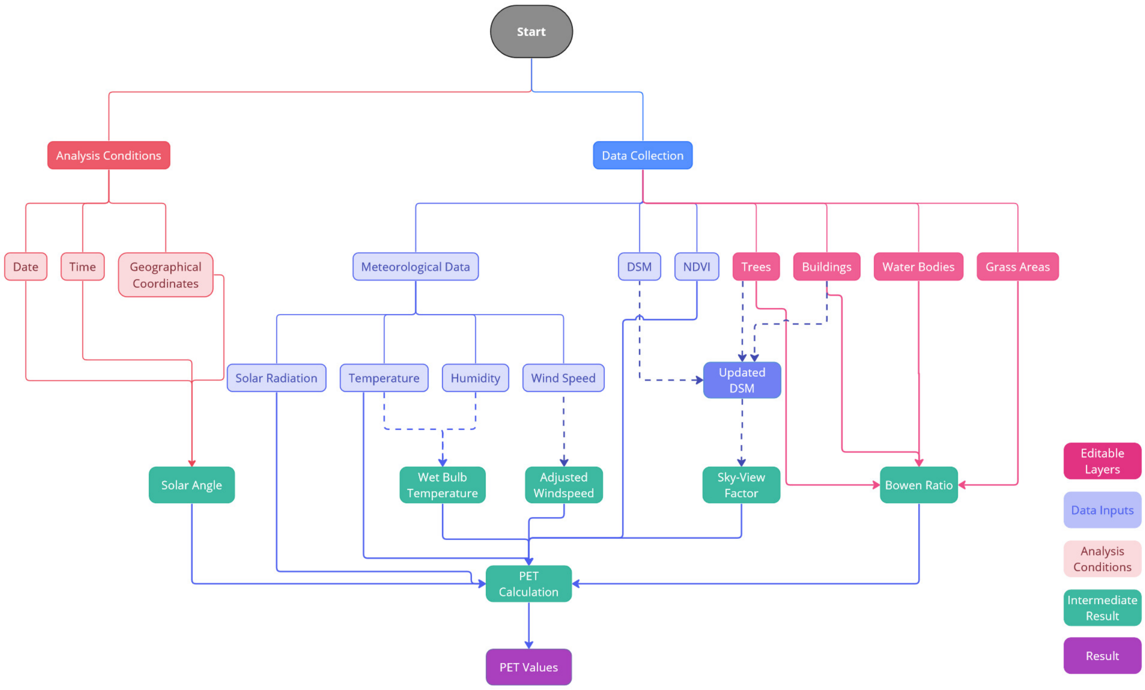

Figure 2. Geo-Processing workflow for PET Calculation. Elements in Magenta can be modified in the editing tools of the Digital Twin.

Figure 3. Polygon ”Stamp” process from points set by the user to duplicated polygons and their rasterization.

values exist and are replaced by the *stamped* trees. This process generates ”new trees”, green areas, and water bodies that appear in the DSM to simulate their effect in the area. It allows users to interactively modify the DSM by adding objects and incorporating them with the building changes for further analysis.

When modifications of the environment are in place, such as adding points representing trees or polygons for vegetation, water areas, or buildings, as explained above, the designed geoprocess integrates the new landscape features and recalculates the PET values for the selected operation window. Table 3 shows the pseudocode the geoprocess follows.

In summary, the process was developed in a local setup, where spatial layers and the geoprocess were initially tested. Afterward, it was integrated into an Online Web service GIS Platform to visualize (2D and 3D) the digital city, where it was possible to incorporate the geospatial data edition tools and the capacity to modify, in real-time, the input on the meteorological conditions of future scenarios or past situations. Additionally, it is possible to execute the geoprocess calculation to obtain a raster that shows the PET values in the user-specified characteristics.

The prototype was presented in a hands-on session to the staff of the Enschede municipality and opened for citizens to engage in an open event at the University of Twente to get to know the operational DT and receive feedback on its usability.

3. Results

Following the abovementioned methodology, the DT tool can be used in 2D and 3D views. The 2D view display lets us observe the city’s current situation regarding street configuration, green areas, blue areas, individual trees, and buildings. When users add elements to the area using the edition panel, these are automatically updated in the database and displayed on the map (see Figure 4a and Figure 4b). Rendering times of 95,976 buildings and 66,350 trees are around 10 sec, depending on the internet speed connection and endpoint user hardware. The edition tools allow for adding green and blue infrastructure, one at a time, and collaborative edition in a Web-based environment.

The 3D visualization was incorporated for better interpretability, enhancing the visualization, and better communicating the changes made to the 2D version in real-time (see Figure 5). This allows users to get a better understanding of their decisions and the integration of new infrastructure with the current environment. The municipality staff and citizens highly appreciated the ability to observe building heights, new green areas, and new water bodies in real-time.

The geoprocessing panel (Figure 6) allows selecting input layers if users want to add their data. The bottom part of the panel allows for the modification of analysis conditions and the execution of the geoprocess. The DT processing is confined to the map extent window the user visualizes to facilitate user interaction and processing times. Wind, DTM, and DSM Raster source data were decided to be kept non-editable due to computational requirements and server limitation of raster processing of up to 4000x4000 pixels per input file.

As a reference, the resulting process shows that the PET values for the selected analysis window and the specified meteorological conditions on the highest recorded temperature day in the 2018-2013 period, as defined in the methodology, are displayed in Figure 7. The PET mean value for this day was 41.63°C (Extreme heat stress) with a maximum of 42.15°C (Extreme heat stress).

Step	Process Description
1	Calculate Wet Bulb Temperature (WB)
2	Calculate Solar Radiation Angle (Solar_Angle)
3	Assign Bowen to Buildings
4	Merge water bodies
5	Dissolve water bodies
6	Add field for water bodies
7	Assign Water Bodies Bowen Ratio
8	Create Water Raster
9	Calculate Field for Grass Areas
10	Convert Grass Areas to Raster
11	Convert Buildings to Raster (Bowen)
12	Reclassify NDVI to Bowen
13	Perform Raster Calculations: - NDVI reclassification - Buildings to Bowen Conditional - Grass + Buildings - Calculate Bowen Ratio
14	Create New Trees
15	Convert Stamped Trees to Raster
16	Convert Buildings to Raster (Height)
17	Create New Buildings Raster
18	Combine Stamped and New Buildings
19	Resample DSM
20	Calculate Sky View Factor (SVF)
21	Calculate Physiological Equivalent Temperature (PET)
Outputs	
1	PET Raster Layer

Table 3. Pseudocode for PET calculation geoprocess

By changing the temperature input in the DT, it was possible to explore future PET values with climate change scenarios of +2 and +4°C, while maintaining the other parameters unexchangeable. As a result, it is possible to observe a change in the PET values in those scenarios if no intervention is made (Figure 8a and Figure 8b). In such scenarios, inside the city center of Enschede, the PET will increase to a mean value of 44.26°C (Extreme heat stress) and a maximum of 44.78°C(Extreme heat stress) in a +2°C scenario; and rise to a mean of 46.89°C (Extreme heat stress) with a maximum of 47.42°C (Most Extreme heat stress) on a +4°C scenario. It is then possible to measure the local impact of such interventions in reducing PET. Figure 9 shows potential reductions of PET up to 1.2°C in the same scenario (2019 conditions) where proposed trees, new green areas, and water bodies were placed. This helps planners understand the benefits of their proposals ex-ante.

The feedback from the city staff's hands-on experience with the DT showed us that using software that the stakeholder group was already familiar with helped with the twin's reception, understanding, and usability. Several participants could interact with the tools in a collaborative environment while only being exposed to a small introductory tutorial, and no programming skills were needed from their side. Additionally, a guide on how to recreate this DT was developed to allow them to understand how it was generated and make further changes and improvements based on advancements in the study of urban heat islands (See Cárdenas et al. (2023)).

4. Discussion

The Digital Twin approach presents a method for easily adopting the standardized model presented by Koopmans et al. (2020). Even though they present detailed supporting material for understanding the method, not every municipality has the technical capacity to develop its calculation process. This DT goes beyond the static

(a) 2D map visualization. Current trees are displayed in light green, while pink trees represent the new proposed trees.

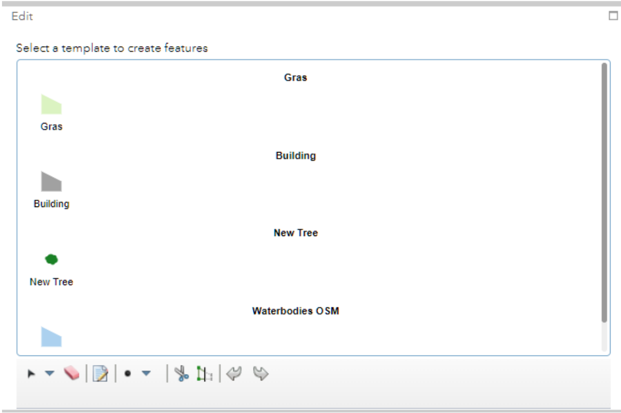

(b) Digital Twin editing panel

Figure 4. Digital Twin for PET calculation

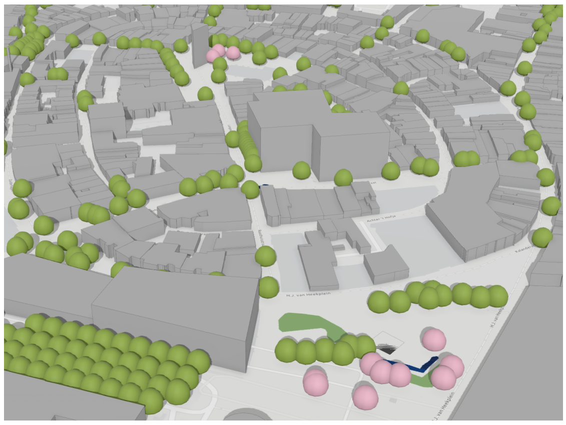

Figure 5. Digital Twin for PET calculation, 3D view. Pink trees represent the new proposed trees in an academic exercise.

analysis on one set of input parameters and allows for testing different scenarios. It gives an easy, online, collaborative platform for users to calculate the PET without the need to revise and recreate the step-by-step method of Koopmans et al. (2020)

The integration of 2D spatial datasets and fast deployment of non-realistic 3D features, along with the real-time editing of the data, was highly appreciated by users. When citizens interacted with the DT, knowledge of their neighborhood and experience became relevant in the scenario testing. Local knowledge of users and placement of new blue and green features gives stakeholders indications on where implementation can be done and its result in the PET values.

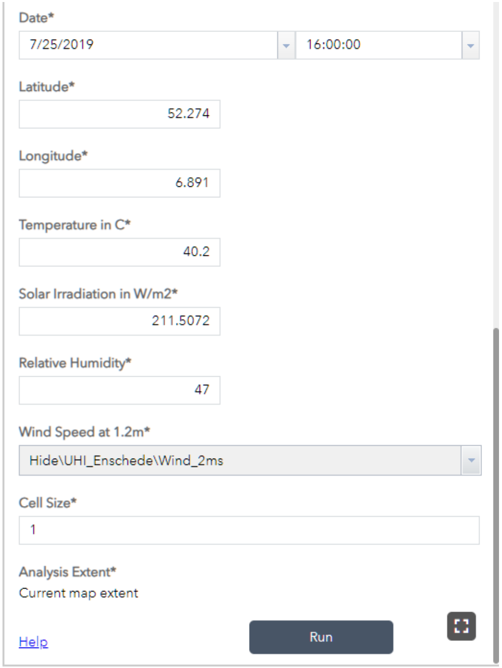

Figure 6. Digital Twin geoprocessing panel. Analysis condition and execution section.

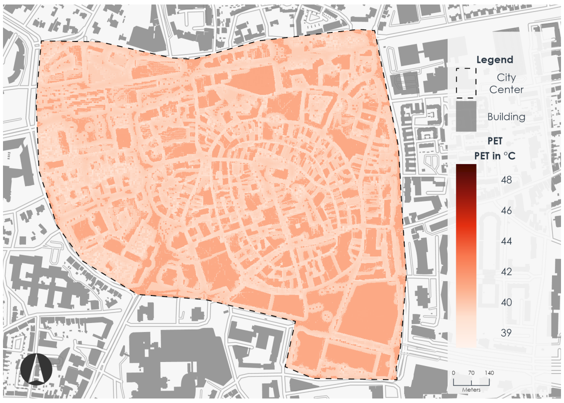

Figure 7. Geoprocessing results showing the PET values for the city center of Enschede on 25th of July 2019.

The simple editing for incorporating trees leaves space for users to determine the location and combination of single individuals. The process is visual and up to the criteria of the user. It does not consider technical decisions and possible conflicts with underground elements or damage to other infrastructure like pipelines, sidewalks, or curbs, as described by (Shi et al., 2023). It can detect possible locations in complex street configurations where some vegetation already exists. It provides a non-symmetric distribution of trees while having the same type of benefits on shade and the reduction in PET that (Yin et al., 2018) presents. The implementation of adding hypothetical trees allowed the placement of different tree crown sizes but not different tree species. Therefore, this could be an enhancement that could be introduced in future updates of the DT, as this could also help identify which species contribute the most to lowering the PET sensation in a specific study area.

Some limitations were present in the development of the twin as the currently available data for the wind at a height of 1.2m is not available in the city of Enschede. Therefore, it was important to develop a practical solution for the regions with similar lack

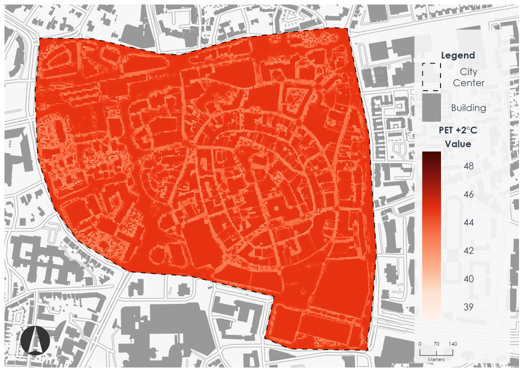

(a) +2°C scenario.

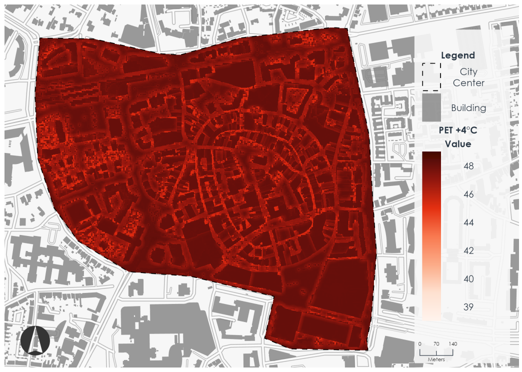

(b) +4°C scenario.

Figure 8. Geoprocessing results showing the PET values for the city center of Enschede.

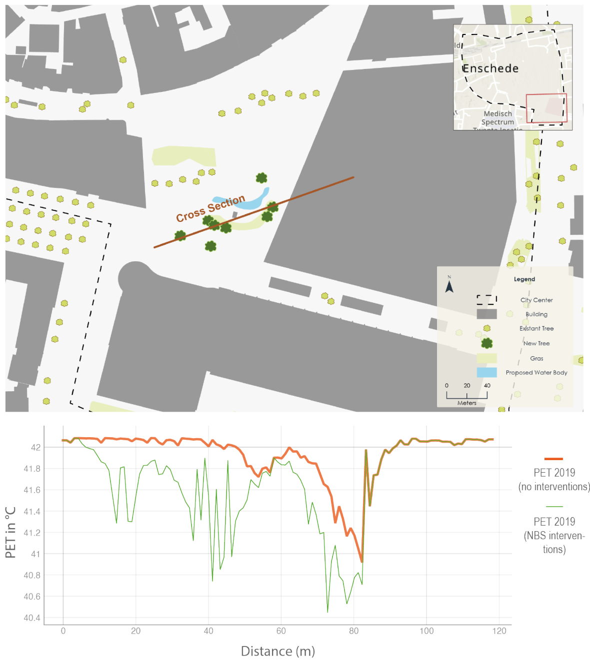

Figure 9. Cross section Detail of citizen proposed intervention with blue and green infrastructure on an area with a large concrete surface in the City Center of Enschede.

of data. To obtain the wind approximation on how the wind was behaving on the day of the warmest temperature in the study area at the specific height that the PET model requires, a wind simulation tool (Windninja) was used (Wagenbrenner et al., 2016). Moreover, WindNinja was selected due to its use of computational fluid dynamics (CFD) to model and predict wind flow patterns and because it is trusted by researchers, scientists, and professionals in various fields, including wildfire management (USDA, 2023), emergency response planning, and wind energy assessment. Therefore, it is noteworthy to make clear that the simulation of wind can introduce some discrepancies in the results obtained with the tool. Therefore, ways to obtain accurate wind speed should be explored to reinforce this part of the model.

The server web-based version of this twin currently works with low-resolution DSM and DTM raster files; this was done due to the need for the results to be generated fast to give the user feedback on how the current changes can affect the modified environment. If the geoprocess is executed outside the cloud configuration, it can generate high-resolution maps in a local setup. However, these results can take up to 5 hours of computational time. Therefore, it is important to continue researching methods to work with higher-resolution files in cloud environments or faster local calculation processes without incurring large investments.

It is also important to highlight that the PET calculation only considers one type of person. This is a Male, 35 years old, 1.75m. Therefore, it is necessary to re-analyze the calculations for other types of people, such as different body weights, women, and especially elders who are the most vulnerable to heat stress (Oudin Åström et al., 2011).

5. Conclusions

The DT developed in this study facilitated the integration of the Physiological Equivalent Temperature indicator for the municipality of Enschede, Netherlands. The design allowed for testing in different climate scenarios and local conditions. Including editing tools in real-time was key for testing small local interventions on the landscape and understanding the consequences this would have before doing any real-world implementation. The PET results of including blue and green infrastructure in the urban environment show their importance for reducing the heat island effect and the subsequent thermal sensation of citizens in urban environments.

The demonstration hands-on sessions in the municipality showed that the DT facilitates stakeholders’ understanding of the predicted scenarios and allows them to obtain vital information on the optimal changes that can reduce the heat island in their city.

Implementing the DT allowed for dynamic visualization and interaction with the city’s digital model, providing stakeholders and citizens with a platform for proposing and evaluating local changes. The developed twin represents a valuable contribution to urban planning, offering a dynamic platform for informed decision-making and community engagement.

6. Acknowledgements

This study was supported by the Vrije Universiteit Amsterdam (VU) and the University of Twente (UT) Collaboration Fund 2022. We want to acknowledge the District Management team from Gemeente Enschede for their input and support on this collaborative design. We thank Lieneke Stam, Marc de Jong, Petra Klein, and Niels Kortenschijl for their help throughout the project.

References

Aguilar, R., 2022. Co-designing planning support tools for stakeholder engagement in collaborative spatial planning processes. PhD Thesis. DOI: http://dx.doi.org/10.3990/1.9789036554206.

Brandsma, T., Wolters, D., 2012. Measurement and Statistical Modeling of the Urban Heat Island of the City of Utrecht (the Netherlands). *Journal of Applied Meteorology and Climatology*, 51(6). DOI: http://dx.doi.org/10.1175/jamc-d-11-0206.1.

Cárdenas, I. L., Morales, R., Koeva, M., Atun, F., Pfeffer, K., 2023. Digital Twins for Physiological Equivalent Temperature Calculation Guide. DOI: http://dx.doi.org/10.5281/ZENODO.8141935.

CBS, 2024. Dataset: Population development; region per month. Technical report, Centraal Bureau voor de Statistiek. https://opendata.cbs.nl/statline/#/CBS/nl/dataset/37230ned/table?ts=1574365385886.

Copernicus Sentinel Data, 2023. Dataset: Harmonized sentinel-2 msi: Multispectral instrument, level-2a. https://developers.google.com/earth-engine/datasets/catalog/COPERNICUS_S2_SR_HARMONIZED#description.

Das, S., Subudhi, S., 2022. A Review on Different Methodologies to Study Thermal Comfort. *International Journal of Environmental Science and Technology*, 19(3), 2155–2171. DOI: http://dx.doi.org/10.1007/s13762-021-03210-8.

Dataset: Actueel Hoogtebestand Nederland 4 (AHN), 2022. Technical report. Accessed: 2023-03-23.

Dataset: Basisregistratie Adressen en Gebouwen (BAG), n.d. https://www.pdok.nl/introductie/-/article/basisregistratie-adressen-en-gebouwen-ba-1. Accessed: 2023-05-04.

Dembski, F., Wössner, U., Letzgus, M., 2019. The Digital Twin Tackling Urban Challenges with Models, Spatial Analysis and Numerical Simulations in Immersive Virtual Environments. *Proceedings of the International Conference on Education and Research in Computer Aided Architectural Design in Europe*, 1, 795–804. DOI: http://dx.doi.org/10.5151/PROCEEDINGS-ECAADESIGRADI2019_334.

Di Bernardino, A., Falasca, S., Iannarelli, A. M., Casadio, S., Siani, A. M., 2023. Effect of heatwaves on urban sea breeze, heat island intensity, and outdoor thermo-hygrometric comfort in Rome (Italy). *Urban Climate*, 52, 101735. DOI: http://dx.doi.org/10.1016/j.uclim.2023.101735.

Digital Twin Geohub, 2022. DIGITAL TWINNING FOR URBAN AND RURAL ENVIRONMENTAL MODELLING. DOI: \protect\relax\itshapeUniversiteitTwente. https://www.utwente.nl/en/digital-society/research/digitalisation/digital-twin-geohub/. Accessed on 2024-03-18.

Feng, L., Yang, S., Zhou, Y., Sun, J., 2024. Optimization strategy of architectural forms to improve the thermal comfort of residential area. *Journal of Building Engineering*, 86, 108905. DOI: http://dx.doi.org/10.1016/j.jobe.2024.108905.

Flacke, J., Aguilar, R., Pfeffer, K., 2022. Citizen participation in Noise Action Planning: Co-designing an open and interactive geospatial tool.

Flynn, A., McGreevy, C., Mulkerrin, E., 2005. Why do older patients die in a heatwave? *QJM: An International Journal of Medicine*, 98(3), 227–229. DOI: http://dx.doi.org/10.1093/qjmed/hci025.

Forthofer, J. M., Butler, B. W., Wagenbrenner, N. S., 2014. A Comparison of Three Approaches for Simulating Fine-Scale Surface Winds in Support of Wildland Fire Management. Part I. Model Formulation and Comparison against Measurements. *International Journal of Wildland Fire*, 23(7), 969–981. DOI: http://dx.doi.org/10.1071/WF12089.

Gemeente Enschede, 2023. Dataset: Bomen, Waterloop, watervlakte.

Gorelick, N., Hancher, M., Dixon, M., Ilyushchenko, S., Thau, D., Moore, R., 2017. Google Earth Engine: Planetary-scale geospatial analysis for everyone. *Remote Sensing of Environment*. DOI: http://dx.doi.org/10.1016/j.rse.2017.06.031.

Höppe, P., 1999. The Physiological Equivalent Temperature – a Universal Index for the Biometeorological Assessment of the Thermal Environment. *International Journal of Biometeorology*, 43(2), 71–75. DOI: http://dx.doi.org/10.1007/s004840050118.

Höppe, P. R., 1993. Heat Balance Modelling. *Experientia*, 49(9), 741–746. DOI: http://dx.doi.org/10.1007/BF01923542.

Jain, M., 2023. Two decades of nighttime surface urban heat island intensity analysis over nine major populated cities of India and implications for heat stress. *Frontiers in Sustainable Cities*, 5. DOI: http://dx.doi.org/10.3389/frsc.2023.1084573.

Kasniza Jumari, N. A. S., Ahmed, A. N., Huang, Y. F., Ng, J. L., Koo, C. H., Chong, K. L., Sherif, M., Elshafie, A., 2023. Analysis of urban heat islands with landsat satellite images and GIS in Kuala Lumpur Metropolitan City. *Heliyon*, 9(8), e18424. DOI: http://dx.doi.org/10.1016/j.heliyon.2023.e18424.

Klok, L., Zwart, S., Verhagen, H., Mauri, E., 2012. The Surface Heat Island of Rotterdam and Its Relationship with Urban Surface Characteristics. *Resources, Conservation and Recycling*, 64, 23–29. DOI: http://dx.doi.org/10.1016/j.resconrec.2012.01.009.

KNMI, 2019. Dataset: Weather Stations Hourly observations. Technical report, Koninklijk Nederlands Meteorologisch Instituut.

Koopmans, S., Heusinkveld, B. G., Steeneveld, G. J., 2020. A standardized Physical Equivalent Temperature urban heat map at 1-m spatial resolution to facilitate climate stress tests in the Netherlands. *Building and Environment*, 181, 106984. DOI: http://dx.doi.org/10.1016/j.buildenv.2020.106984.

Koopmans, S., Ronda, R., Steeneveld, G.-J., Holtslag, A., Klein Tank, A., 2018. Quantifying the Effect of Different Urban Planning Strategies on Heat Stress for Current and Future Climates in the Agglomeration of The Hague (The Netherlands). *Atmosphere*, 9(9), 353. DOI: http://dx.doi.org/10.3390/atmos9090353.

Matzarakis, A., Mayer, H., 1996. Another Kind of Environmental stress: Thermal Stress.

McGregor, G. R., Nieuwolt, S. et al., 1998. *Tropical climatology: an introduction to the climates of the low latitudes.* John Wiley & Sons Ltd.

OpenStreetMap contributors, 2023. OpenStreetMap database [PostgreSQL via API]. OpenStreetMap Foundation. ©OpenStreetMap contributors. Available under the Open Database Licence from: http://openstreetmap.org. Data mining by Overpass turbo. Available at http://overpass-turbo.eu.

Oudin Åström, D., Bertil, F., Joacim, R., 2011. Heat wave impact on morbidity and mortality in the elderly population: A review of recent studies. *Maturitas*, 69(2), 99–105. DOI: http://dx.doi.org/10.1016/j.maturitas.2011.03.008.

Pauly, L., Canonico, M., Ferrero, E., 2024. Numerical investigation of thermal patterns and local wind circulations to characterize Urban Heat Island during a heatwave in Turin. *Urban Climate*, 54, 101847. DOI: http://dx.doi.org/10.1016/j.uclim.2024.101847.

Ruohomaki, T., Airaksinen, E., Huuska, P., Kesaniemi, O., Martikka, M., Suomisto, J., 2018. Smart City Platform Enabling Digital Twin. *9th International Conference on Intelligent Systems 2018: Theory, Research and Innovation in Applications, IS 2018 - Proceedings*, 155–161. DOI: http://dx.doi.org/10.1109/IS.2018.8710517.

Shi, F., Meng, Q., Pan, L., Wang, J., 2023. Root damage of street trees in urban environments: An overview of its hazards, causes, and prevention and control measures. *Science of The Total Environment*, 904, 166728. DOI: http://dx.doi.org/10.1016/j.scitotenv.2023.166728.

Sidiqui, P., Roös, P. B., Herron, M., Jones, D. S., Duncan, E., Jalali, A., Allam, Z., Roberts, B. J., Schmidt, A., Tariq, M. A. U. R., Shah, A. A., Khan, N. A., Irshad, M., 2022. Urban Heat Island vulnerability mapping using advanced GIS data and tools. *Journal of Earth System Science*, 131(4), 266. DOI: http://dx.doi.org/10.1007/s12040-022-02005-w.

Tong, S., Prior, J., McGregor, G., Shi, X., Kinney, P., 2021. Urban heat: an increasing threat to global health. *BMJ*, 375, n2467. DOI: http://dx.doi.org/10.1136/bmj.n2467. Publisher: British Medical Journal Publishing Group Section: Analysis.

USDA, 2023. WindNinja. https://weather.firelab.org/windninja/faq.html. Accessed:2024-01-29.

Valmassoi, A., Keller, J. D., 2021. How to visualize the Urban Heat Island in Gridded Datasets? *Advances in Science and Research*, 18, Copernicus GmbH, 41–49. ISSN: 1992-0628.

Wagenbrenner, N. S., Forthofer, J. M., Lamb, B. K., Shannon, K. S., Butler, B. W., 2016. Downscaling surface wind predictions from numerical weather prediction models in complex terrain with WindNinja. preprint, Dynamics/Atmospheric Modelling/Troposphere/Physics (physical properties and processes).

Xi, Y., Wang, S., Zou, Y., Zhou, X., Zhang, Y., 2024. Seasonal Surface Urban Heat Island Analysis Based on Local Climate Zones. *Ecological Indicators*, 159, 111669. DOI: http://dx.doi.org/10.1016/j.ecolind.2024.111669.

Yin, C., Yuan, M., Lu, Y., Huang, Y., Liu, Y., 2018. Effects of urban form on the urban heat island effect based on spatial regression model. *Science of The Total Environment*, 634, 696–704. DOI: http://dx.doi.org/10.1016/j.scitotenv.2018.03.350.

Zhang, L., Liu, H., Wei, D., Liu, F., Li, Y., Li, H., Dong, Z., Cheng, J., Tian, L., Zhang, G., Shi, L., 2022. Impacts of Spatial Components on Outdoor Thermal Comfort in Traditional Linpan Settlements. *International Journal of Environmental Research and Public Health*, 19(11), 6421. DOI: http://dx.doi.org/10.3390/ijerph19116421.

Zhao, H., Fang, Y., Xu, X., 2024. Quantifying morphology evolutions of urban heat islands and assessing their heat exposure in a metropolis. *Sustainable Cities and Society*, 102, 105244. DOI: http://dx.doi.org/10.1016/j.scs.2024.105244.

Zou, M., Zhang, H., 2021. Cooling strategies for thermal comfort in cities: a review of key methods in landscape design. *Environmental Science and Pollution Research*, 28(44), 62640–62650. DOI: http://dx.doi.org/10.1007/s11356-021-15172-y.

Çağlak, S., 2024. A new model approach to mapping bioclimatic comfort conditions. *Theoretical and Applied Climatology*. DOI: http://dx.doi.org/10.1007/s00704-023-04816-3.